Mineralogical Magazine (2019), **83**, 233–238
doi:10.1180/mgm.2018.139

CAMBRIDGE UNIVERSITY PRESS

Article

Agmantinite, Ag_2MnSnS_4, a new mineral with a wurtzite derivative structure from the Uchucchacua polymetallic deposit, Lima Department, Peru

Frank N. Keutsch[1]*, Dan Topa[2], Rie Takagi Fredrickson[3], Emil Makovicky[4] and Werner H. Paar[5]

[1]John A. Paulson School of Engineering and Applied Sciences and Department of Chemistry and Chemical Biology, Harvard University, Cambridge, MA 02138, USA; [2]Naturhistorisches Museum-Wien, Burgring 7, 1010 Wien, Austria; [3]Department of Chemistry, University of Wisconsin-Madison, WI 53706, USA; [4]Institute for Geoscience and Natural Resource Management, Østervoldgade 10, DK-1350, Copenhagen K, Denmark; and [5]Fachbereich Chemie und Physik der Materialien, University, Hellbrunnerstr. 34, A-5020 Salzburg, Austria (Department of chemistry and physics of materials)

Abstract

Agmantinite, ideally Ag_2MnSnS_4, is a new mineral from the Uchucchacua polymetallic deposit, Oyon district, Catajambo, Lima Department, Peru. It occurs as orange–red crystals up to 100 μm across. Agmantinite is translucent with adamantine lustre and possesses a red streak. It is brittle. Neither fracture nor cleavage were observed. Based on the empirical formula the calculated density is 4.574 g/cm^3. On the basis of chemically similar compounds the Mohs hardness is estimated at between 2 to 2½. In plane-polarised light agmantinite is white with red internal reflections. It is weakly bireflectant with no observable pleochroism with red internal reflections. Between crossed polars, agmantinite is weakly anisotropic with reddish brown to greenish grey rotation tints. The reflectances (R_{min} and R_{max}) for the four standard wavelengths are: 19.7 and 22.0 (470 nm); 20.5 and 23.2 (546 nm); 21.7 and 2.49 (589 nm); and 20.6 and 23.6 (650 nm), respectively.

Agmantinite is orthorhombic, space group $P2_1nm$, with unit-cell parameters: $a = 6.632(2)$, $b = 6.922(2)$, $c = 8.156(2)$ Å, $V = 374.41(17)$ Å^3, a:b:c 0.958:1:1.178 and $Z = 2$. The crystal structure was refined to $R = 0.0575$ for 519 reflections with $I > 2\sigma(I)$. Agmantinite is the first known mineral of $M^{I}_2M^{II}M^{IV}S_4$ type that is derived from wurtzite rather than sphalerite by ordered substitution of Zn, analogous to the substitution pattern for deriving stannite from sphalerite. The six strongest X-ray powder-diffraction lines derived from single-crystal X-ray diffraction data [d in Å (intensity)] are: 3.51 (s), 3.32 (w), 3.11 (vs), 2.42 (w), 2.04 (m) and 1.88 (m). The empirical formula (based on 8 apfu) is $(Ag_{1.94}Cu_{0.03})_{\Sigma 1.97}(Mn_{0.98}Zn_{0.05})_{\Sigma 1.03}Sn_{0.97}S_{4.03}$.The crystal structure-derived formula is $Ag_2(Mn_{0.69}Zn_{0.31})_{\Sigma 1.00}SnS_4$ and the simplified formula is Ag_2MnSnS_4.

The name is for the composition and the new mineral and mineral name have been approved by the International Mineralogical Association Commission on New Minerals, Nomenclature and Classification (IMA2014-083).

Keywords: agmantinite, new mineral, electron-microprobe data, reflectance data, X-ray diffraction data, wurtzite, stannite, Uchucchacua deposit, Peru

(Received 20 April 2016; accepted 25 May 2018)

Introduction

There are numerous minerals with the $M^{I}_2M^{II}M^{IV}S_4$ composition that are derived from the sphalerite structure by ordered substitution of Zn. These are divided into the stannite group (space group $I\bar{4}2m$) with briartite, $Cu_2(Fe,Zn)GeS_4$ (Wintenberger 1979, synthetic), černýite, Cu_2CdSnS_4 (Szymanski *et al.*, 1978), stannite, Cu_2FeSnS_4 (Hall *et al.*, 1978) and velikite, Cu_2HgSnS_4 (Kaplunik *et al.*, 1977), and the kësterite subgroup (space group $I\bar{4}$) with ferrokësterite, Cu_2FeSnS_4 (Kissin and Owens, 1989), hocartite, Ag_2FeSnS_4 (Caye *et al.*, 1968, structure not solved), kësterite, Cu_2ZnSnS_4 (Hall *et al.*, 1978), pirquitasite, Ag_2ZnSnS_4 (Schumer *et al.*, 2013) and zincobriartite, $Cu_2(Zn,Fe)(Ge,Ga)S_4$ (McDonald *et al.*, 2016). The two subgroups have two distinct but closely related patterns of ordered substitution of the Zn atoms in sphalerite. In the stannite-subgroup minerals, (001) layers of Zn atoms are substituted by layers of Cu atoms which alternate with layers in which Zn atoms are substituted by ordered (M^{II}+M^{IV}) atoms, whereas, in the kësterite subgroup, (001) layers of Zn atoms are substituted by layers of ordered (M^{I}+M^{II}) atoms which alternate with layers in which Zn atoms are substituted by ordered (M^{I}+M^{IV}) atoms. Iron is the only M^{II} case for which both types of structures have been found as minerals (stannite/ferrokësterite). There are closely related minerals $M^{I}_2M^{I}M^{V}S_4$, which include luzonite Cu_2CuAsS_4 (Marumo *et al.*, 1967), famatinite Cu_2CuSbS_4 (Garin and Parthé, 1972, synthetic), and keutschite Cu_2AgAsS_4 (Topa *et al.*, 2014). Some uncertainty remains with respect to the structures of other $M^{I}_2M^{II}M^{IV}S_4$ minerals, as the structure of barquillite Cu_2CdGeS_4 has not been determined using single-crystal methods (Murciego *et al.*,

*Author for correspondence: Frank N. Keutsch, Email: keutsch@seas.harvard.edu
Associate Editor: David Hibbs
Cite this article: Keutsch F.N., Topa D., Fredrickson R.T., Makovicky E. and Paar W.H. (2019) Agmantinite, Ag_2MnSnS_4, a new mineral with a wurtzite derivative structure from the Uchucchacua polymetallic deposit, Lima Department, Peru. *Mineralogical Magazine* **83**, 233–238. https://doi.org/10.1180/mgm.2018.139

1999) for the natural occurrence, and synthetic Cu_2CdGeS_4 has a wurtzite/enargite derived structure related to agmantinite (Parthé *et al.*, 1969). Uncertainty also remains with respect to the structures of kuramite and petrukite. Synthetic compounds with $M^{I}_2M^{II}M^{IV}S_4$ composition derived from the wurtzite ZnS structure are known, including Cu_2MnGeS_4 and Cu_2MnSiS_4 (Bernert and Pfitzner, 2005), but no such cases have been reported previously for minerals. The only mineral of $M^{I}_2M^{I}M^{V}S_4$ type derived via ordered substitution of Zn in wurtzite is enargite, Cu_2CuAsS_4 (Karanovic *et al.*, 2002), a dimorph of luzonite.

In this paper we report occurrence, physical properties and crystal structure of agmantinite (ideally, Ag_2MnSnS_4), which is the first mineral with $M^{I}_2M^{II}M^{IV}S_4$ composition derived from the wurtzite ZnS structure. It was found in one sample from the alabandite zone of the Uchucchacua polymetallic deposit, Oyon district, Lima Department, Peru. The mineral was named for its composition and the new mineral and mineral name have been approved by the International Mineralogical Association Commission on New Minerals, Nomenclature and Classification (IMA2014-083, Keutsch *et al.*, 2015). Holotype material is deposited in the reference collection of the Naturhistorisches Museum Wien, Wien, Austria, specimen number N 9736.

Occurrence and physical properties

The sample with agmantinite was found during a study of the mineralogy of the Uchucchacua polymetallic deposit that focuses on a zone with high Ag and Mn content. This zone is characterised by the occurrence of alabandite and silver minerals. Uchucchacua is the type locality for six Mn-bearing sulfides/sulfosalts: uchucchacuaite, $AgPb_3MnSb_5S_{12}$ (Moëlo *et al.*, 1984); benavidesite, $Pb_4MnSb_6S_{14}$ (Oudin *et al.*, 1982); manganoquadratite, $AgMnAsS_3$ (Bonazzi *et al.*, 2012); menchettiite, $AgPb_{2.40}Mn_{1.60}Sb_3As_2S_{12}$ (Bindi *et al.*, 2012); oyonite, $Ag_3Mn_2Pb_4Sb_7As_4S_{24}$ (Bindi *et al.*, 2018); agmantinite, Ag_2MnSnS_4 (this work); and including keutschite, Cu_2AgAsS_4 (Topa *et al.*, 2014) and spryite, $Ag_8(As^{3+}, As^{5+})S_6$ (Bindi *et al.*, 2017). It is the type locality of seven silver minerals, as well as being the type locality of hyršlite, $Pb_8As_{10}Sb_6S_{32}$ (Keutsch *et al.*, 2017). Geological and metallogenetic data concerning the Uchucchacua deposit district have been reported by Oudin *et al.* (1982).

The sample with agmantinite consists mainly of calcite and quartz with associated minor manganoquadratite, alabandite, proustite, probable kutnohorite, sphalerite and Pb–Sb–As–S minerals. Agmantinite occurs as extremely rare translucent, orange–red, flattened, free-standing crystals rarely reaching 100 μm on small quartz and calcite crystals with small manganoquadratite crystals as the only other minerals in direct association (Fig. 1). It is the least common mineral discovered in the course of the study of the alabandite zone in Uchucchacua, and despite exhaustive searches only one sample with two groups of small crystals has been discovered.

Agmantinite is orange–red in colour and has a red streak. The mineral is translucent with adamantine lustre. It is brittle. No fracture or cleavage was observed in the material available. Due to the small crystal size the density could not be measured. Based on the empirical formula the calculated density is 4.574 g/cm^3. The microhardness could not be determined. On the basis of chemically similar compounds the Mohs hardness is estimated to be in the range of 2 to 2½.

In plane-polarised light, agmantinite is greyish white with no discernible pleochroism and weak bireflectance. With crossed polars, the mineral is weakly anisotropic (air) in reddish brown to greenish rotation tints. Agmantinite has red internal reflections. Reflectance measurements were made within the visible spectrum (400–700 nm) at intervals of 20 nm using a Leitz MPV-SP microscope-spectrophotometer. A WTiC reflectance standard (Zeiss 314) was used as the reference. The measurements were performed on an untwined grain with a ×50 objective, the effective numerical apertures of which were confined to 0.28, and the diameters of the measured discs were 10 μm. The results are presented in Table 1. The spectra of agmantinite are unique and cannot be compared to members of the stannite and kësterite subgroups.

The reflectance spectra obtained for agmantinite and compared to those of pirquitasite, Ag_2ZnSnS_4 (Johan and Picot, 1982) is shown in Fig. 2. There is an obvious increase of R of agmantinite up to a maximum at 600 nm whereas R of pirquitasite decreases. In the region after $R = 600$ nm the behaviour of both minerals is similar (reflectance decreases). At 600 nm the bireflectance of agmantinite is twice as large as for pirquitasite.

Fig. 1. Photograph of part of the type specimen showing agmantinite crystals on quartz and manganoan calcite. The typical orange–red colour and habit can be seen in the two main crystals, which are viewed from two different directions. The size of the largest crystal is 100 μm. Naturhistorisches Museum Wien, specimen number N 9736.

Table 1. Reflectance data for agmantinite

λ (nm)	R_{min}	R_{max}	λ (nm)	R_{min}	R_{max}
400	19.0	19.7	560	20.5	23.4
420	19.4	21.9	580	21.1	24.3
440	19.4	21.9	**589**	**21.7**	**24.9**
460	19.5	21.7	600	21.5	25.0
470	**19.7**	**22.0**	620	21.4	24.3
480	19.7	22.0	640	20.9	23.9
500	19.9	22.5	**650**	**20.6**	**23.6**
520	20.2	22.8	660	20.3	23.2
540	20.4	23.0	680	19.7	22.7
546	**20.5**	**23.2**	700	19.6	22.5

The reference wavelengths required by the Commission on Ore Mineralogy (COM) are given in bold.

https://doi.org/10.1180/mgm.2018.139 Published online by Cambridge University Press

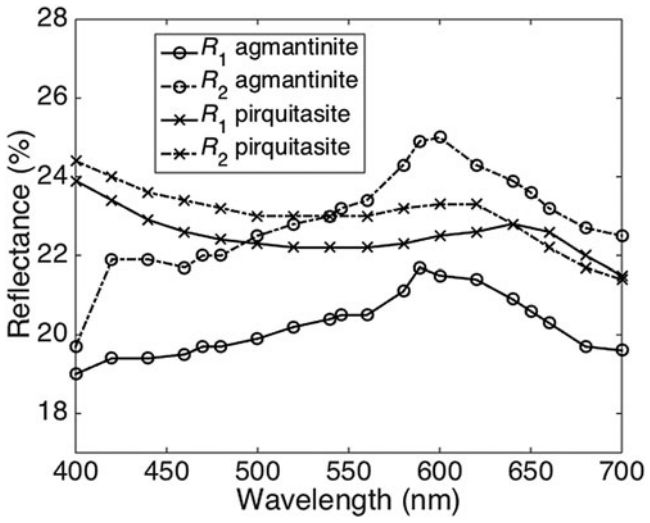

Fig. 2. Reflectance spectra (air) for agmantinite and pirquitasite (Johan and Picot 1982).

X-ray crystallography and crystal-structure determination

A crystal fragment of agmantinite with irregular shape and 0.05 mm × 0.04 mm × 0.03 mm in size was selected from the rock sample and examined by means of a Bruker AXS three-circle diffractometer equipped with a CCD area detector using graphite-monochromatised Mo*K*α radiation. The *SMART* (Bruker AXS, 1998*a*) system of programs was used for unit-cell determination and data collection, *SAINT*+ (Bruker AXS, 1998*b*) for the reduction of the intensity data, and *XPREP* (Bruker AXS, 1997) for space-group determination and empirical absorption correction based on pseudo ψ-scans. The non-centrosymmetric space group $P2_1nm$ proposed by the *XPREP* program was chosen. The structure of agmantinite was solved by direct methods (Sheldrick, 1997*a*), which revealed most of the atom positions. In subsequent cycles of the refinement (Sheldrick, 1997*b*), remaining atom positions were deduced from difference-Fourier syntheses by selecting from among the strongest maxima at appropriate distances. The structure of agmantinite contains one Ag site, one Sn site, one mixed Mn(Zn) site and three S sites. Atom coordinates and anisotropic displacement parameters are given in Table 2, bond lengths and bond angles in Table 3. The amount of Zn in the mixed site (occupancy value) is higher than in the empirical chemical formula, indicating a possible variation of the Mn/Zn ratio from grain to grain. Crystal data and a summary of parameters describing data collection and refinement for agmantinite are given in Table 4.

Powder X-ray diffraction data were derived from measurements of the same single-crystal specimen on an Oxford Diffraction Xcalibur E diffractometer using graphite-

Table 4. Details of data collection and refinement.

Crystal data	
X-ray formula	$Ag_2(Mn_{0.69}Zn_{0.31})_{\Sigma 1.00}SnS_4$
Crystal dimensions (mm^3)	0.05×0.04×0.03
Crystal system, space group	Orthorhombic, $P2_1nm$
a, *b*, *c* (Å)	6.632(2), 6.922(2), 8.156(2)
V (Å^3)	374.7(2)
Z	2
D_{calc} (g cm^{-3})	4.608
Data collection and refinement	
Crystal colour	Orange–red
Crystal habit	Irregular
Instrument diffractometer	Bruker AXS three-circle
Radiation, wavelength (Å)	Mo*K*α, 0.71073
Data collection temperature (K)	300
Absorption coefficient (mm^{-1})	11.380
$2\theta_{min}$, $2\theta_{max}$	5.88, 46.66
Absorption correction	Phi and omega scans
Number of reflections [$I > 2\sigma(I)$, all]	533, 519
Indices range of *h*, *k*, *l*	$-7 \le h \le 7$, $-7 \le k \le 7$, $-9 \le l \le 9$
Refinement	
Refinement method	F^2
R_{int} [$I > 2\sigma(I)$]	9.26
Number of refined parameters	45
R_1 [$I > 2\sigma(I)$], wR_2 [$I > 2\sigma(I)$]	5.75, 17.36
R_1 [all], wR_2 [all]	5.79, 17.41
GoF = *S* [$I > 2\sigma(I)$, *S* (all)]	1.22, 1.22
$\Delta\rho_{max}$, $\Delta\rho_{min}$ (e^- Å^{-3})	2.134, −2.164

Table 2. Final atom coordinates and U_{eq} values (Å^2) and anisotropic displacement parameters (Å^2).

Atom	Occupancy	*x*/*a*	*y*/*b*	*z*/*c*	U_{eq}	U^{11}	U^{22}	U^{33}	U^{23}	U^{13}	U^{12}
Sn	1	0.6480(10)	0.3225(3)	0	0.0267(9)	0.0149(19)	0.0325(12)	0.0327(13)	0.000	0.000	−0.0111(14)
Ag	1	0.13855(1)	0.1672(2)	0.2506(2)	0.0235(8)	0.0196(18)	0.0287(10)	0.0223(10)	0.0018(5)	−0.0056(14)	0.0027(15)
Mn/Zn	0.69/0.31	0.1630(12)	0.6547(6)	0	0.040(3)	0.014(6)	0.052(4)	0.056(4)	0.000	0.000	−0.010(4)
S1	1	0.0142(14)	0.3174(10)	0	0.0175(18)	0.014(4)	0.013(4)	0.0025(5)	0.000	0.000	−0.014(3)
S2	1	0.5255(15)	0.6544(9)	0	0.0178(18)	0.033(5)	0.009(3)	0.011(4)	0.000	0.000	−0.013(3)
S3	1	0.5161(15)	0.1684(8)	0.2440(6)	0.0261(16)	0.032(4)	0.030(4)	0.017(4)	0.0033(19)	−0.009(2)	−0.007(2)

Table 3. Selected bond lengths (Å) and angles (°) in agmantinite.

Sn–S1	2.429(10)	Sn–S2	2.437(8)	Sn–S3	2.422(7)	Sn–S3	2.422(7)
Ag–S1	2.437(5)	Ag–S2	2.495(4)	Ag–S3	2.462(6)	Ag–S3	2.504(10)
Mn–S1	2.534(8)	Mn–S2	2.404(13)	Mn–S3	2.609(7)	Mn–S3	2.609(7)
S3–Sn–S3	110.5(3)	S3–Sn–S1	110.8(2)	S3–Sn–S2	107.1(2)	S2–Sn–S1	110.3(3)
S3–Ag–S3	109.5(2)	S3–Ag–S1	107.8(2)	S3–Ag–S2	110.7(3)	S2–Ag–S1	111.8(2)
S3–Mn–S3	106.3(3)	S3–Mn–S1	106.7(3)	S3–Mn–S2	111.9(3)	S2–Mn–S1	112.9(4)

https://doi.org/10.1180/mgm.2018.139 Published online by Cambridge University Press

monochromatised Mo*K*α radiation (λ = 0.7107 Å) at ambient temperature. Observed intensities were added for different 2θ values and *d* spacings were calculated from these. The data obtained had broad peaks (full width at half maximum ~0.08) but showed good consistency with the intensities and *d* spacings calculated using *Jade9* (v9.5.0, MDI Materials Data, California, USA, 2012) software on the basis of the structural model (see below); only calculated reflections with $I > 1$ are reported (if not observed). Observed intensities were estimated visually; vs = very strong; s = strong; m = medium; w = weak. Data (in Å for Mo*K*α) are listed in Table 5.

Chemical composition

The chemical composition of an agmantinite grain (Fig. 3) was determined using wavelength dispersive analysis (WDS) by a JEOL Hyperprobe JXA-8530F field-emission electron microprobe, installed at Natural History Museum, Vienna, Austria (25 kV, 20 nA, beam size = 2 μm); standards used (element): pure metal (Ag); chalcopyrite (Cu); hauerite (Mn); sphalerite (Zn); pure metal (Sn); and sphalerite (S). No other elements with atomic number >11 were detected. The chemical compositions (four analyses on one grain) are reported in Table 6. The chemical formula, $(Ag_{1.94}Cu_{0.03})_{\Sigma 1.97}(Mn_{0.98}Zn_{0.05})_{\Sigma 1.03}Sn_{0.97}S_{4.03}$, was calculated on the basis of 8 atoms. The ideal formula is Ag_2MnSnS_4.

Description of the structure and discussion

The crystal structure of agmantinite (Fig. 4) is derived from that of wurtzite by ordered substitution of Zn. This substitution pattern is analogous to that for deriving stannite from sphalerite. In stannite (001) layers of sphalerite Zn atoms are substituted by layers of Cu atoms alternating with layers in which Zn atoms are substituted by ordered (Fe + Sn) atoms [in contrast to kësterite, in which (001) layers of Zn atoms are substituted by layers of ordered (Cu + Zn/Fe) which alternate with layers of Zn atoms that are substituted by ordered (Cu + Sn)]. Analogously to stannite, in agmantinite, layers of Zn atoms are substituted by layers of Ag atoms in alternation with layers in which Zn atoms are substituted by ordered (Sn + Mn/Zn) atoms, but starting with the wurtzite ZnS structure rather than the sphalerite one. These substitutions proceed on alternating (001) cation levels. The substitution results in an orthorhombic unit cell and an increase of unit-cell dimensions compared to the corresponding dimensions in wurtzite. The corresponding dimensions in wurtzite are $a = 6.188$, $b = 6.542$ and $c = 7.554$ Å, whereas those in agmantinite are $a = 6.632$, $b = 6.922$ and $c = 8.156$ Å. Although not obvious from Fig. 4, Ag tetrahedra are situated on (001) planes at about ¼ and ¾ *c*; Ag–S distances are 2.50 Å along the *a* direction whereas they appear to adjust to the differences in atomic radii of Mn^{2+} and Sn^{4+} in the (100) plane: 2.44 Å towards S bound to Sn in the adjacent [100] Sn–Mn populated columns (in the (001) plane, Sn–S bonds are equal to 2 × 2.42 Å and 2.44 Å) and 2.50 Å towards Mn in these columns (in this plane Mn–S bonds are equal to 2 × 2.61 Å and 2.54 Å). The remaining Ag–S bond, subparallel to the *b* direction, towards S in the adjacent Ag populated [100] column, is 2.46 Å, a compromise between similarly oriented 2.54 Å and 2.44 Å bonds of Mn and Sn with S, respectively. Along *a*, Sn^{4+} preserves a regular

Table 5. Measured and calculated powder X-ray diffraction data*.

obs**	I_{calc}	2θ	d^{obs}/Å	d_{calc}/Å	*hkl*
	1	5.875		6.92	010
	9	7.702		5.28	011
	9	7.893		5.15	101
	4	8.498		4.79	110
	1	9.846		4.13	111
	1	9.961		4.08	002
s	63, 34	11.572, 11.766	3.51	3.514, 3.461	012, 020
w	68	12.283	3.32	3.316	200
vs	100, 46	13.098, 13.280	3.11	3.105, 3.068	112, 120
	2	14.185		2.8717	121
	3	14.507		2.8078	211
	1	15.824		2.5728	202
	1	16.090		2.5305	013
	1	16.176		2.5155	103
	2	16.620		2.4518	122
w	25, 13	16.893, 17.042	2.42	2.4116, 2.3944	212, 220
	1	19.397		2.1053	131
m	23, 1, 43	19.999, 20.275, 20.340	2.04 broad	2.0390, 2.0117, 2.0081	004, 213, 032
m	45, 21	21.833, 21.956	1.88	1.87114, 1.86305	312, 320
	7	23.265		1.75679	024
m	15, 2, 29, 12	23.515, 23.659, 23.820, 24.072	1.73	1.73693, 1.73043, 1.71771, 1.69822	204, 040, 232, 124
	6	24.464		1.67437	140
	3	24.710		1.65803	400
	5	26.371		1.55239	224
	2	26.742		1.53411	240
	2	27.347		1.49946	412
	11	29.844		1.37539	324

*The theoretical pattern was calculated with *PowderCell 2.3* software (Kraus and Nolze, 1999) in Debye-Scherrer configuration with Mo*K*α radiation (λ = 0.7107 Å), a fixed slit, and no anomalous dispersion. Cell parameters, space group, atom positions, site-occupancy factors and isotropic displacement factors from the crystal-structure determination were used.
**s = very strong; m = medium; w = weak

https://doi.org/10.1180/mgm.2018.139 Published online by Cambridge University Press

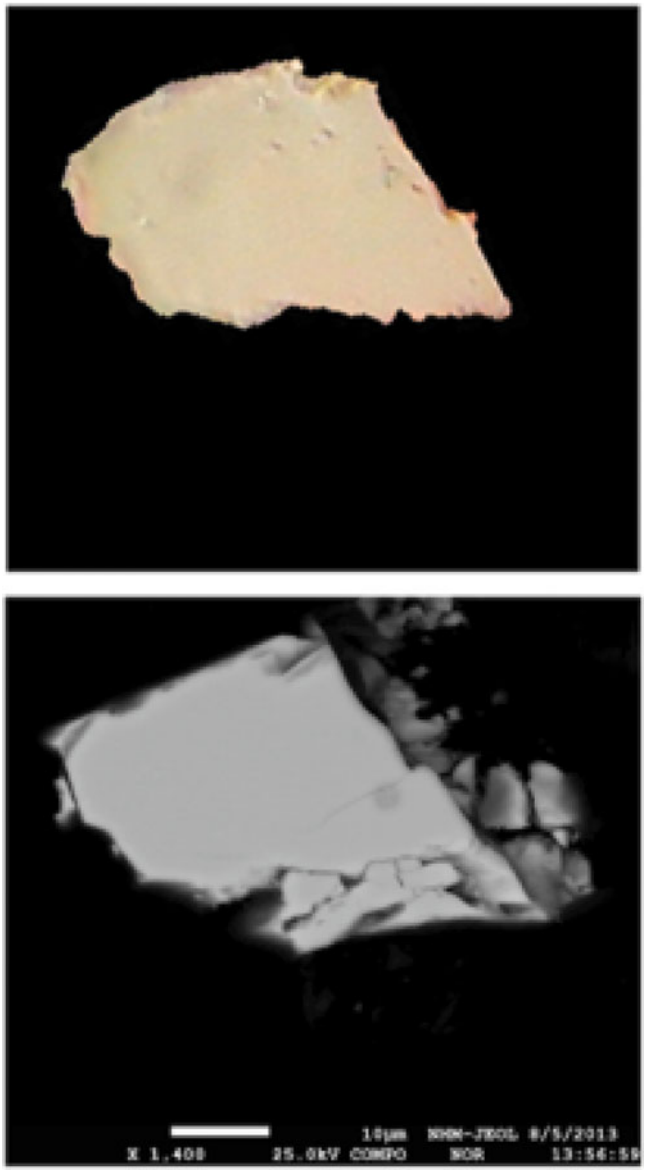

Fig. 3. Secondary electron image of an agmantinite grain and its optical image under crossed polars. Scale bar = 10 μm.

Table 6. Analytical data for agmantinite.

	Wt.%	Range	S.D.	Standards and lines
Ag	40.87	40.71–41.02	0.15	Metal (syn.) Ag*Lα*
Cu	0.42	0.39–0.45	0.02	Chalcopyrite (nat.) Cu*Kα*
Mn	10.53	9.92–10.78	0.41	Hauerite (nat.) Mn*Kα*
Zn	0.62	0.33–1.34	0.48	Sphalerite (nat.) Zn*Kα*
Sn	22.56	22.37–22.77	0.18	Metal (syn.) Sn*Lα*
S	25.25	25.22–25.29	0.03	Sphalerite (nat.) S*Kα*
Total	100.25			

S.D. = standard deviation.

tetrahedral coordination, with the Sn–S distance equal to 2.43 Å, whereas Mn has a short distance of 2.40 Å and Ag the longest one, 2.50 Å; they display small distortions of their tetrahedral coordination, but with the opposite sense. Although $M^{I}_{2}M^{II}M^{IV}S_4$ compounds are common minerals, the structure of agmantinite is the first example of a $M^{I}_{2}M^{II}M^{IV}S_4$ type mineral that is derived from the wurtzite structure and not sphalerite. However, synthetic $M^{I}_{2}M^{II}M^{IV}S_4$ phases derived from the wurtzite structure have been described, including those of Cu_2MnGeS_4 and Cu_2MnSiS_4 (Bernet and Pfitzner, 2005), and enargite, Cu_2CuAsS_4, of $M^{I}_{2}M^{I}M^{V}S_4$ type is derived from the wurtzite structure.

The mineral adds to the list of Ag- and Mn-bearing minerals described from the Uchucchacua deposit. In addition, during study of the alabandite zone other minerals chemically related to agmantinite, such as stannite, këstерite and keutschite were found. The Uchucchacua deposit is unusual for the occurrence of Ag–Mn bearing minerals (uchucchacuaite, manganoquadratite, menchettiite, oyonite and agmantinite) and Mn-bearing sulfosalts (benavidesite, in addition to those listed above). The only Mn-bearing sulfosalts so far not encountered during the study within the alabandite zone at Uchucchacua are clerite and samsonite. Investigations of the exotic mineralogy of the 'alabandite zone' are ongoing and will possibly result in the description of new and chemically and structurally exciting species.

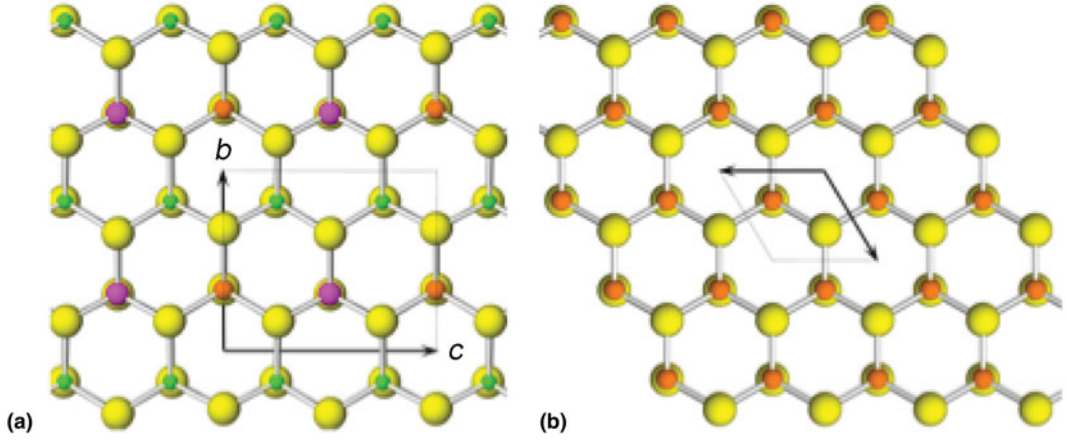

Fig. 4. The crystal structure of agmantinite (*a*) viewed along [100]; yellow: S sites, green: Ag sites, magenta: Sn sites, brown: Mn(Zn) sites and (*b*) the crystal structure of wurtzite viewed along [001]; yellow: S sites, brown: Zn sites.

https://doi.org/10.1180/mgm.2018.139 Published online by Cambridge University Press

Acknowledgements. The authors thank Daniel Fredrickson (University of Wisconsin-Madison, USA) for helpful discussions and Christian Rewitzer (Furth im Wald, Germany) for taking the photograph of agmantinite.

Supplementary material. To view supplementary material for this article, please visit https://doi.org/10.1180/mgm.2018.139

References

Bernert T. and Pfitzner A. (2005) $Cu_2MnM^{IV}S_4$ (M^{IV} = Si, Ge, Sn) – analysis of crystal structures and tetrahedra volumes of normal tetrahedral compounds. *Zeitschrift für Kristallographie*, **220**, 968–972.

Bindi L., Keutsch F.N. and Bonazzi P. (2012) Menchettiite, $AgPb_{2.40}Mn_{1.60}Sb_3As_2S_{12}$, a new sulfosalt belonging to the lillianite series from the Uchucchacua polymetallic deposit, Lima Department, Peru. *American Mineralogist*, **97**, 440–446.

Bindi L., Keutsch F.N., Morana M. and Zaccarini F. (2017) Spryite, $Ag_8(As^{3+}_{0.5}As^{5+}_{0.5})S_6$: structure determination and inferred absence of superionic conduction of the first As^{3+}-bearing argyrodite. *Physics and Chemistry of Minerals*, **44**, 75–82.

Bindi L., Biagioni C. and Keutsch F.N. (2018) Oyonite, $Ag_3Mn_2Pb_4Sb_7As_4S_{24}$, a new member of the lillianite homologous series from the Uchucchacua base-metal deposit, Oyon District, Peru. *Minerals*, **8**, 192.

Bonazzi P, Keutsch F.N. and Bindi L. (2012) Manganoquadratite, $AgMnAsS_3$, a new manganese-bearing sulfosalt from the Uchucchacua polymetallic deposit, Lima Department, Peru: Description and crystal structure. *American Mineralogist*, **97**, 1199–1205.

Bruker AXS (1997) *SHELXTL, Version 5.1*. Bruker AXS, Inc., Madison, WI 53719, USA.

Bruker AXS (1998*a*) *SMART, Version 5.0*. Bruker AXS, Inc., Madison, WI 53719, USA.

Bruker AXS (1998*b*) *SAINT, Version 5.0*. Bruker AXS, Inc., Madison, WI 53719, USA.

Caye R., Laurent Y., Picot P., Pierrot R. and Levy C. (1968) La hocartite, Ag_2SnFeS_4, une nouvelle espece minerale. *Bulletin de la Société française de Minéralogie et de Cristallographie*, **91**, 383–387.

Garin J. and Parthé E. (1972) The crystal structure of Cu_3PSe_4 and other ternary normal tetrahedral structure compounds with composition 1_356_4. *Acta Crystallographica*, **B28**, 3672–3674.

Hall S.R., Szymanski J.T. and Stewart J.M. (1978) Kësterite, $Cu_2(Zn,Fe)SnS_4$, and stannite, $Cu_2(Fe,Zn)SnS_4$, structurally similar but distinct minerals. *The Canadian Mineralogist*, **16**, 131–137.

Johan Z. and Picot P. (1982) La pirquitasite, Ag_2ZnSnS_4, un nouveau member du groupe de la stannite. *Bulletin de Minéralogie*, **105**, 229–235.

Kaplunnik L.N., Pobedimskaya E.A. and Belov N.V. (1977) Crystal structure of velikite $Cu_{3.75}Hg_{1.75}Sn_2S_8$. *Soviet Physics Crystallography*, **22**, 99–100.

Karanovic L., Cvetkovic L., Balić-Žunić T. and Makovicky E. (2002) Crystal and absolute structure of enargite form Bor (Serbia). *Neues Jahrbuch fuer Mineralogie-Monatshefte*, **6**, 241–253.

Keutsch F.N., Topa D., Takagi Fredrickson R., Makovicky E. and Paar W. (2015) Agmantinite, IMA 2014-083. CNMNC Newsletter No. 23, February 2015, page 57; *Mineralogical Magazine*, **79**, 51–58.

Keutsch F.N., Topa D. and Makovicky E. (2017) Hyršlite, IMA 2016-097. CNMNC Newsletter No. 36, April 2017, page 404; *Mineralogical Magazine*, **81**, 403–409.

Kissin S.A. and Owens D.R. (1989) The relatives of stannite in the light of new data. *The Canadian Mineralogist*, **27**, 673–688.

Kraus W. and Nolze G. (1999) *Powder Cell for Windows, version 2.3*. BAM, Berlin, Germany.

Marumo F. and Nowacki W. (1967) A refinement of the crystal structure of luzonite, Cu_3AsS_4 *Zeitschrift fur Kristallographie* **124**, 1–8.

McDonald A.M., Stanley C.J., Ross K.C. and Nestola F. (2016) Zincobriartite, IMA 2015-094. CNMNC Newsletter No. 29, February 2016, page 203; *Mineralogical Magazine*, **80**, 199–205.

Moëlo Y., Oudin E., Picot P. and Caye R. (1984) L'uchucchacuaite, $AgMnPb_3Sb_5S_{12}$, une nouvelle espece minerale de la serie de l'andorite. *Bullettin de Minéralogie*, **107**, 597–604.

Murciego A., Pascua M.I., Babkine J., Dusausoy Y., Medenbach O. and Bernhardt H.-J. (1999) Barquillite, $Cu_2(Cd, Fe)GeS_4$, a new mineral from the Barquilla deposit, Salamanca, Spain. *European Journal of Mineralogy*, **11**, 111–117.

Oudin E., Picot P., Pillard F., Moëlo Y., Burke E. and Zakrzewski A. (1982) La benavidesite, $Pb_4(Mn,Fe)Sb_6S_{14}$, un nouveau mineral de la serie de la jamesonite. *Bullettin de Minéralogie*, **105**, 166–169.

Parthé E., Yvon K. and Deitch R.H. (1969) The crystal structure of Cu_2CdGeS_4 and other quaternary normal tetrahedral structure compounds. *Acta Crystallographica*, **B25**, 1164–1174.

Schumer B.N., Downs R.T., Domanik K.J., Andrade M.B. and Origlieri M.J. (2013) Pirquitasite, Ag_2ZnSnS_4. *Acta Crystallographica*, **E69**, i8–i9.

Sheldrick G.M. (1997*a*) *SHELXS-97. A computer program for crystal structure determination*. University of Göttingen, Germany.

Sheldrick G.M. (1997*b*) *SHELXL-97. A computer program for crystal structure refinement*. University of Göttingen, Germany.

Szymanski J.T. (1978) The crystal structure of Černýite, Cu_2CdSnS_4, a cadmium analogue of stannite. *The Canadian Mineralogist*, **16**, 147–151.

Topa D., Fredrickson R.T. and Stanley C. (2014) Keutschite, IMA 2014-038. CNMNC Newsletter No. 21, August 2014, page 804. *Mineralogical Magazine*, **78**, 797–804.

Wintenberger M. (1979) Etude de la structure cristallographique et magnetique de Cu_2FeGeS_4 et remarque sur la structure magnetique de Cu_2MnSnS_4. *Materials Research Bulletin*, **14**, 1195–1202.